

1 Composition and light absorption of N-containing aromatic compounds
2 in organic aerosols from laboratory biomass burning

3

4 Mingjie Xie^{1,2,3,4,*}, Xi Chen⁴, Michael D. Hays⁴, Amara L. Holder⁴

5

6 ¹Collaborative Innovation Center of Atmospheric Environment and Equipment Technology,
7 Jiangsu Key Laboratory of Atmospheric Environment Monitoring and Pollution Control, School
8 of Environmental Science and Engineering, Nanjing University of Information Science &
9 Technology, 219 Ningliu Road, Nanjing 210044, China

10 ²State Key Laboratory of Pollution Control and Resource Reuse, School of the Environment,
11 Nanjing University, Nanjing, China

12 ³Oak Ridge Institute for Science and Education (ORISE), Office of Research and Development,
13 U.S. Environmental Protection Agency, 109 T.W. Alexander Drive, Research Triangle Park, NC
14 27711, USA

15 ⁴National Risk Management Research Laboratory, Office of Research and Development, U.S.
16 Environmental Protection Agency, 109 T.W. Alexander Drive, Research Triangle Park, NC
17 27711, USA

18

19

20 *Correspondence to: Mingjie Xie

21 E-mail: mingjie.xie@colorado.edu; mingjie.xie@nuist.edu.cn;

22 Tel: +86-18851903788;

23 Fax: +86-25-58731051;

24 Mailing address: 219 Ningliu Road, Nanjing, Jiangsu, 210044, China

25

26

27

28

29

30 **ABSTRACT**

31 This study seeks to understand the compositional details of N-containing aromatic
32 compounds (NACs) emitted during biomass burning (BB) and their contribution to light-
33 absorbing organic carbon (OC), also termed brown carbon (BrC). Three laboratory BB
34 experiments were conducted with two U.S. pine forest understory fuels typical of those
35 consumed during prescribed fires. During the experiments, submicron aerosol particles were
36 collected on filter media and subsequently extracted with methanol and examined for their
37 optical and chemical properties. Significant correlations ($p < 0.05$) were observed between BrC
38 absorption and elemental carbon (EC)/OC ratios for individual burns data. However, the pooled
39 experimental data indicated that EC/OC alone cannot explain the BB BrC absorption. Fourteen
40 NAC formulas were identified in the BB samples, most of which were also observed in
41 simulated secondary organic aerosol (SOA) from photo-oxidation of aromatic VOCs with NO_x .
42 However, the molecular structures associated with the identical NAC formula from BB and SOA
43 are different. In this work, the identified NACs from BB are featured by methoxy and cyanate
44 groups, and are predominately generated during the flaming phase. The mass concentrations of
45 identified NACs were quantified using authentic and surrogate standards, and their contributions
46 to bulk light absorption of solvent extractable OC were also calculated. The contributions of
47 identified NACs to organic matter (OM) and BrC absorption were significantly higher in
48 flaming-phase samples than those in smoldering-phase samples, and correlated with EC/OC ratio
49 ($p < 0.05$) for both individual burns and pooled experimental data, indicating that the formation
50 of NACs from BB largely depends on burn conditions. The average contributions of identified
51 NACs to overall BrC absorption at 365 nm ranged from 0.087 ± 0.024 to $1.22 \pm 0.54\%$, 3 – 10
52 times higher than their mass contributions to OM (0.023 ± 0.0089 to $0.18 \pm 0.067\%$), so the

53 NACs with light absorption identified in this work from BB are likely strong BrC chromophores.
54 Further studies are warranted to identify more light-absorbing compounds to explain the
55 unknown fraction (> 98%) of BB BrC absorption.

56

57 **1 Introduction**

58 Biomass burning (BB), including residential burning for cooking, heating, and open
59 burning, is a major source of atmospheric carbonaceous aerosol, contributing 62% and 93% of
60 black carbon (BC) and primary organic carbon (OC) particle emissions, respectively (Bond et al.,
61 2004). BC can absorb sunlight across the entire spectral range with a weak dependence on
62 wavelength (λ) (Bond, 2001; Bond et al., 2013; Lack and Langridge, 2013). OC in particulate
63 matter (PM) is commonly treated as purely light scattering component in global climate models
64 (Chung et al., 2002; Myhre et al., 2013). Recent field and laboratory studies found that the light
65 absorption of BB OC increases rapidly from the purple-green region (400–550 nm) to near
66 ultraviolet (UV) region (300–400 nm) (Kirchstetter et al., 2004; Laskin et al., 2015; Chakrabarty
67 et al., 2016; Xie et al., 2017b). The light absorption and scattering by BC and OC from BB can
68 directly affect the Earth's radiative balance (Ramanathan et al., 2001; Anderson et al., 2003; Bond
69 and Bergstrom, 2006), and BC emission factors and its warming effect have been intensively
70 investigated (Bond et al., 2004; Bond et al., 2013). However, the optical properties and chemical
71 composition of light-absorbing OC, also termed brown carbon (BrC) from BB is less well
72 characterized. The chromophores in BrC are expected to have high degree of unsaturation or
73 conjugation (Chen and Bond, 2010; Lin et al., 2014; Laskin et al., 2015), but are seldom identified
74 and used as BrC tracers in the atmosphere (Desyaterik et al., 2013; Zhang et al., 2013; Teich et al.,
75 2016).

76 Polycyclic aromatic hydrocarbons (PAHs) and their derivatives are typical BrC
77 chromophores (Samburova et al., 2016;Huang et al., 2018), of which the light absorption in the
78 UV and visible wavelength range is highly dependent on ring numbers and degree of conjugation
79 (Samburova et al., 2016). However, PAH emissions are not source-specific, but are associated
80 with multiple different combustion processes, including BB (Samburova et al., 2016), coal
81 burning (Chen et al., 2005), motor vehicle emissions (Riddle et al., 2007), etc. Therefore, PAHs
82 are not unique to BB BrC. N-containing aromatic compounds (NACs) are another class of BrC
83 chromophores that have been detected in BB (Lin et al., 2016), cloud water (Desyaterik et al.,
84 2013) and atmospheric particles (Zhang et al., 2013;Teich et al., 2017). In water extracts of
85 atmospheric particles, NACs can contribute greater than 3% of the light absorption at 365–370
86 nm (Zhang et al., 2013;Teich et al., 2017). These results suggest that NACs are important BrC
87 chromophores, but their composition and structures are less certain for BB aerosols.
88 Nitrophenols, nitrocatechols, and methyl nitrocatechols (including isomers) are commonly
89 observed in BB aerosols (Iinuma at al., 2010; Claeys et al., 2012;Lin et al., 2016;Lin et al., 2017),
90 and are also generated from the photo-oxidation of benzene, toluene, and *m*-creosol in the
91 presence of NO_x (Iinuma et al., 2010;Lin et al., 2015;Xie et al., 2017a). As such, other NAC
92 structures specific to BB are needed to represent BB BrC chromophores. Additionally, very few
93 studies have examined the influence of burn conditions on the formation of NACs in BB
94 emissions, although it is well known that increasing combustion temperature, or flaming
95 dominated combustion, is associated with strong BrC absorption (Chen and Bond, 2010;Saleh et
96 al., 2014).

97 The present study attempts to characterize the compositional profile of NACs from BB,
98 identify additional NAC structures in laboratory BB samples, and evaluate the contributions of

99 NACs to bulk absorption of solvent extractable OC from BB. A high-performance liquid
100 chromatograph interfaced to a diode array detector (HPLC/DAD) and quadrupole (Q)-time-of-
101 flight mass spectrometer (ToF-MS) was used to examine NACs in PM_{2.5} (particulate matter with
102 aerodynamic diameter $\leq 2.5 \mu\text{m}$) from three BB experiments. A thermal-optical instrument
103 determined bulk OC and elemental carbon (EC) in the PM, and a UV/Vis spectrometer was used
104 to measure total BrC absorption in methanol extracts of BB PM_{2.5}. In this work, a number of
105 NACs formulas with structures that might be specifically related to BB were identified, and the
106 contributions of identified NACs to bulk BrC absorption were calculated. These results shed
107 light on the light-absorbing characteristics of BB OC at bulk chemical and molecular levels,
108 benefiting the understanding of BrC sources and chromophores.

109 **2 Methods**

110 **2.1 Laboratory open BB simulations**

111 Laboratory simulations of open BB were conducted at the U.S. EPA [Research Triangle
112 Park (RTP), North Carolina (NC)] Open Burn Test Facility (OBTF), a 70 m³ enclosure, as
113 detailed in Grandesso et al. (2011). Details of the protocols for biomass fuel collection and burn
114 simulations were provided elsewhere (Aurell and Gullett, 2013; Aurell et al., 2015; Holder et al.,
115 2016). Briefly, forest understory fuels were gathered from two different locations in the
116 southeastern United States — Florida (FL) and NC. The FL forest field (Eglin Air Force Base,
117 FL) is characteristic of a well-managed long leaf pine (*Pinus palustris*) ecosystem. The NC
118 forest was located near the EPA campus in RTP, and it contained mainly Loblolly pine (*Pinus*
119 *taeda*) with some deciduous hardwood trees leaf litter. Biomass fuel was divided by a quartering
120 procedure (Aurell and Gullett, 2013) and burned in batches (1 kg) on an aluminum foil-coated
121 steel pan (1 m \times 1 m). Ambient air was pulled into the OBTF through a large inlet at ground

122 level and the combustion exhaust was drawn through a roof duct near a baghouse using a high-
123 volume blower. PM_{2.5} was sampled at 10 L min⁻¹ on Teflon (47 mm, Pall, Ann Arbor, Michigan,
124 USA) and pre-heated (550 °C, 12 h) quartz filters (QF, diameter 43 mm, Pall) with a PM_{2.5}
125 impactor (SKC, Pittsburgh, Pennsylvania, USA). For the NC forest fire simulation, filter samples
126 were collected during an initial flaming phase lasting approximately 1–3 minutes. After most of
127 the flames were extinguished, a second set of filter samples were obtained for the smoldering
128 emissions. Smoldering samples were collected until there was little or no visible smoke being
129 emitted from the fuel bed, typically lasting 6–15 minutes. Two separate experiments were done
130 with the NC forest fuels in spring and summer, respectively, with different ambient temperatures
131 (Table S1). Sampling of the FL forest fire simulations was done in autumn over the complete
132 burn, not by combustion phase. Only one experiment was done for the FL forest fuels collected
133 in fall. Background samples were obtained post-burn inside the OBTF. A summary of the sample
134 information is provided in Table S1 of the supporting information.

135 **2.2 Bulk carbon and light absorption measurement**

136 Details of the bulk OC, EC and light absorption analysis methods are provided in Xie et
137 al. (2017a,b). Briefly, the bulk OC and EC were measured using an OC-EC analyzer (Sunset
138 Laboratories, Portland, OR) with a modified NIOSH method 5040 protocol (NIOSH, 1999). For
139 light absorption measurement, one filter punch (1.5 cm²) was extracted in 5 mL methanol (HPLC
140 grade) ultrasonically for 15 min, and then filtered through a 30 mm diameter
141 polytetrafluoroethylene (PTFE) filter with a 0.2 µm pore size (National Scientific Company).
142 The light absorption of methanol extracts was measured with a UV/Vis spectrometer (V660,
143 Jasco Incorporated, Easton MD) over the wavelength range of 200 to 900 nm. To ensure data
144 quality, the wavelength accuracy (± 0.3 nm) and repeatability (± 0.05 nm) were tracked every

145 month with a NIST traceable Holmium Oxide standard. Solvent background was subtracted with
146 a reference cuvette containing pure methanol. The extracted filter was air dried in a fume hood
147 overnight, and the residual OC was measured with the Sunset thermal-optical analyzer. The
148 extraction efficiency (η , %) of OC by methanol is calculated by:

$$149 \quad \eta = \frac{OC_b - OC_r}{OC_b} \times 100\% \quad (1)$$

150 where OC_b is the OC content of $PM_{2.5}$ filter before extraction and OC_r is the OC content in the
151 air dried filter after extraction.

152 The light absorption coefficient of the methanol extracts (Abs_λ , Mm^{-1}) is calculated as:

$$153 \quad Abs_\lambda = (A_\lambda - A_{700}) \times \frac{V_l}{V_a \times L} \ln(10) \quad (2)$$

154 where A_{700} is subtracted from A_λ to correct baseline drift, V_l (m^3) is the solvent volume (5 mL)
155 used for extraction, V_a (m^3) is the air volume of the extracted filter area, L (0.01 m) is the optical
156 path length, and $\ln(10)$ converts the absorption coefficient in units of m^{-1} from log base-10 to
157 natural log (Hecobian et al., 2010). The bulk mass absorption coefficient (MAC_λ , $m^2 gC^{-1}$) is
158 calculated by:

$$159 \quad MAC_\lambda = \frac{Abs_\lambda}{C_{OC}} \quad (3)$$

160 where C_{OC} is the mass concentration of extractable OC ($OC_b - OC_r$) for each filter sample ($\mu g m^{-3}$).
161 The solution absorption Ångström exponent (\mathring{A}_{abs}) is determined from the slope of the linear
162 regression of $\log_{10}(Abs_\lambda)$ vs. $\log_{10}(\lambda)$ over the λ range of 300 to 550 nm. In the current work,
163 Abs_λ and MAC_λ were focused at 365 nm and 550 nm, representing the BrC absorption at near
164 UV and visible regions (Zhang et al., 2013; Saleh et al., 2014), respectively. The EC/OC ratio,
165 methanol extraction efficiency (η) and light-absorbing properties (Abs_λ , MAC_λ and \mathring{A}_{abs}) of each
166 BB sample are listed in Table S1 and summarized in Table 1.

167 **2.3 Filter extraction and HPLC/DAD-Q-ToFMS analysis**

168 The PM_{2.5} filter extraction and subsequent instrumental analysis methods used here are
169 the same as those described in Xie et al. (2017a). Briefly, a 4–6 cm² piece of each filter was pre-
170 spiked with 25 μL of 10 ng μL⁻¹ nitrophenol-d4 (internal standard, IS), and extracted
171 ultrasonically in 3–5 mL of methanol twice (15 min each). After filtration and concentration, the
172 final volume was roughly 500 μL prior to HPLC/DAD-Q-ToFMS analysis. An Agilent 1200
173 series HPLC equipped with a Zorbax Eclipse Plus C18 column (2.1×100 mm, 1.8 μm particle
174 size, Agilent Technologies) was used to separate the target NACs with an injection volume of 2
175 μL. The flow rate of the column was set at 0.2 mL min⁻¹, and the gradient separation was
176 conducted with 0.2% acetic acid (v/v) in water (eluent A) and methanol (eluent B). The
177 concentration of eluent B was 25% for the first 3 min, increased to 100% from 3 to 10 min, held
178 at 100% from 10 to 32 min, and then decreased back to 25% from 32 to 37 min. The
179 identification and quantification of NACs were determined with an Agilent 6520 Q-ToFMS. The
180 Q-ToFMS was equipped with a multimode ion source operating in electrospray ionization (ESI)
181 and negative (–) ion modes. All samples were analyzed in full scan mode (40–1000 Da), and an
182 acceptance criterion of ± 10 ppm mass accuracy was set for compound identification and
183 quantification. Then selected samples were re-examined using collision-induced dissociation
184 (CID) technique under identical chromatographic conditions. The MS/MS spectra of target [M–
185 H][–] ions provided *m/z* data, which was used for identifying NAC structures.

186 The extracted ion chromatograms (EICs) and Q-ToF MS/MS spectra for identified
187 compounds in selected BB samples are provided in Fig. S1 of the supplementary information and
188 Fig. 1, respectively. The Q-ToF MS/MS spectra of standard and surrogate compounds used in
189 this work are obtained from Xie et al. (2017a) and provided in Fig. S2 for comparison. Table 2

190 provides the formulas, standard/surrogate assignments, and proposed structures of the identified
191 NACs. Due to the lack of authentic standards, most of the NACs in BB samples were quantified
192 using surrogates in this work. In general, the surrogate compound with similar molecular weight
193 (MW) and/or structure was selected for the mass quantification of each identified NAC. Since
194 the standard compound with hydroxyphenyl cyanate structure is not commercially available,
195 $C_8H_7NO_4$ and $C_9H_9NO_4$ were quantified as 2-methyl-5-nitrobenzoic acid ($C_8H_7NO_4$) and 2,5-
196 dimethyl-4-nitrobenzoic acid ($C_9H_9NO_4$), respectively; all the identified NACs with MW > 200
197 Da were quantified as 2-nitrophenol ($C_6H_5NO_2$). The mass quantification was conducted
198 using the internal standard method with 9-point calibration curves ($\sim 0.01\text{--}2\text{ ng }\mu\text{L}^{-1}$). The
199 compounds corresponding to each NAC formula (including isomers) were quantified
200 individually and added together for the calculation of mass contribution (%) to organic matter
201 ($\text{OM }\mu\text{g m}^{-3}$) in each sample. The quality assurance and control (QA/QC) procedures applied for
202 NACs quantification were provided in Xie et al. (2017a). Field blank and background samples
203 were free of contamination for NACs. Average recoveries of standard compounds ranged from
204 75.1 to 116%, and the method detection limit ranged from 0.70 to 17.6 pg (Table S2).

205 **3 Results and discussion**

206 **3.1 Light absorption of extractable OC**

207 The average EC/OC ratio, OC extraction efficiency, MAC_{365} , MAC_{550} , and $\mathring{A}_{\text{abs}}$ of all
208 samples grouped by experiment and fire phase are shown in Table 1. Abbreviations for each
209 sample group are also listed in the table. The optical properties and bulk composition of the FL
210 forest samples were reported in Xie et al. (2017b). The average extraction efficiency for all
211 groups of BB samples is greater than 95% (range 97.0 ± 1.87 to $99.5 \pm 0.33\%$), and the light
212 absorption exhibits strong wavelength dependence, with average $\mathring{A}_{\text{abs}}$ values ranging from $5.68 \pm$

213 0.70 to 7.95 ± 0.22 . For each of the two NC forest experiments, the samples collected during the
214 flaming phase (NF1 and NF2) have significantly higher (student's t test, $p < 0.05$) average
215 EC/OC ratios, MAC_{365} and MAC_{550} , and lower ($p < 0.05$) \dot{A}_{abs} than those collected during the
216 smoldering phase (NS1 and NS2). When combining the results from the two NC forest
217 experiments, the average MAC_{365} values for NC forest 2 are significantly ($p < 0.05$) higher than
218 NC forest 1, despite having a comparable EC/OC ratio (NF1 = 0.042 ± 0.014 and NF2 = $0.049 \pm$
219 0.011 , NS1 = 0.0098 ± 0.0024 and NS2 = 0.0075 ± 0.0026). Additionally, the average EC/OC
220 ratio of FF samples is 5–30 times higher than NF and NS samples, while the average MAC_{365}
221 and MAC_{550} values of FF samples (1.13 ± 0.15 and $0.053 \pm 0.023 \text{ m}^2 \text{ gC}^{-1}$) are comparable to
222 NS1 samples (1.10 ± 0.11 and $0.054 \pm 0.015 \text{ m}^2 \text{ gC}^{-1}$), but lower than other NC forest samples.

223 High temperature pyrolysis or intense flaming conditions are known to increase the
224 fraction of EC in the total carbonaceous aerosol emissions of BB (Hosseini et al., 2013; Eriksson
225 et al., 2014; Martinsson et al., 2015; Nielsen et al., 2017). Several studies found that the light-
226 absorbing properties of BB OC could be parameterized as a function of the EC/OC or
227 BC/organic aerosol (OA) ratio, a measurement proxy for burn conditions (McMeeking et al.,
228 2014; Saleh et al., 2014; Lu et al., 2015; Pokhrel et al., 2016), and inferred that the absorptivity of
229 BB OC depended strongly on burn conditions, not fuel type. In Xie et al. (2017b), significant
230 correlations ($p < 0.05$) between MAC_{365} of methanol extractable OC from BB and EC/OC ratios
231 were observed only for samples with identical fuel type, but not for pooled samples with
232 different fuel types, indicating that both burn conditions and fuel types can impact the light
233 absorption of BB OC. The contradiction is possibly ascribed to different approaches used in
234 characterizing the light absorption of BB OC and different test fuel types (Xie et al., 2017b). In
235 the current work, we combined the sample measurements from all three BB experiments and

236 analyzed the correlations of bulk MAC_{365} vs. EC/OC . For the analysis, we removed one FL
237 forest experiment sample due to the extremely high EC/OC ratio of 0.58 (burn 3, Table S1).
238 Generally, EC/OC ratios are < 0.4 for laboratory BB (Akagi et al., 2011; Pokhrel et al., 2016; Xie
239 et al., 2017b), and ≤ 0.1 for field BB (Aurell et al., 2015; Xie et al., 2017b; Zhou et al., 2017).
240 Thus, the burn condition of the FL forest burn 3 (Table S1) is unrepresentative of laboratory BB
241 simulations or field BB. In Fig. 2a, the bulk MAC_{365} of methanol-extracted OC correlated
242 significantly ($p < 0.05$) with EC/OC for each BB experiment. However, grouping these sample
243 measurements resulted in no correlation between MAC_{365} and EC/OC ratio (Fig. 2b). Similar
244 results were also observed for MAC_{550} vs. EC/OC and \hat{A}_{abs} vs. EC/OC correlations (Fig. S3a–d).
245 These results supported that BB BrC absorption depended on more than fire conditions, and
246 light-absorbing components can be formed at relatively low EC/OC (e.g., tar balls) from
247 smoldering biomass combustion (Chakrabarty et al., 2010).

248 In this work, both the comparison of the flaming versus smoldering samples for each
249 NC experiment (Table 1) and the regressions of bulk MAC_{365} versus EC/OC for individual burns
250 (Fig. 2a) suggest that the light absorption of OC from BB is strongly dependent on burn
251 conditions when the fuel type and ambient conditions are similar. The comparison of the FL
252 versus NC forest experiments (Table 1) and the relationship between bulk MAC_{365} and EC/OC
253 for grouped measurements (Fig. 2b) indicate that the burn conditions are not the only factor
254 impacting BB OC absorption. The two NC forest experiments were conducted in spring and
255 summer, respectively, with distinct ambient conditions (Table S1), and their average MAC_{365}
256 values were significantly ($p < 0.05$) different. This could be partly ascribed to the fact that more
257 semi-volatile OC (SVOC) will partition into gas phase in summer with higher ambient
258 temperatures, and the SVOC is less light-absorbing than OC with low volatility (Chen et al.,

259 2010;Saleh et al., 2014). However, if the relative abundance of EC and OC from BB emissions is
260 similar between the two NC forest experiments, the evaporation of SVOCs in summer will lead
261 to higher EC/OC ratios, which is not observed in Table 1. No previous study investigated the
262 seasonal variation in BrC absorption from BB with similar fuel type. Chen et al. (2001) found
263 that the ambient temperature might play a role in EC production from traffic by changing the air
264 density. We suspected that the BB samples from NC forest 2 combustion in summer contained
265 much stronger light-absorbing components than NC forest 1 combustion in spring, although the
266 formation mechanism of these strong BrC components is uncertain and merits further study.
267 Therefore, the light absorption of BB OC is influenced by factors other than burn conditions, and
268 EC/OC ratios alone may not predict BB OC light absorption from burns with varying fuel types
269 and ambient conditions.

270 **3.2 Identification and quantification of NACs**

271 In the current work, fourteen NAC chemical formulas in BB samples were identified
272 (Table 2) using the HPLC/DAD-Q-ToFMS analysis, covering all the NACs with high abundance
273 and strong absorption in ambient and BB particles reported in previous work (Claeys et al.,
274 2012;Mohr et al., 2013;Zhang et al., 2013;Chow et al., 2016;Lin et al., 2016;Lin et al., 2017).
275 Their EICs are provided in Fig. S1. The NACs structures corresponding to each chemical
276 formula were examined using MS/MS data in Fig. 1. In Table S3, the averages and ranges of
277 relative mass contributions of identified NACs to OM are provided by BB experiment and burn
278 condition. Here the OM mass was calculated as $1.7 \times \text{OC mass}$ (Reff et al., 2009). In addition,
279 the average relative mass contributions of each NAC in BB samples are shown in Fig. 3.

280 The three BB experiments have consistent mass contribution profiles (Fig. 3), although
281 they used different fuel types and were conducted in different seasons. In Table S3, the BB

282 samples collected during flaming periods (NF1 and NF2) contain significantly higher ($p < 0.05$)
283 average relative mass contributions from total NACs to OM (tNAC_{OM}%: NF1 $0.18 \pm 0.067\%$,
284 NF2 $0.16 \pm 0.045\%$) than those collected during smoldering periods (NS1 $0.055 \pm 0.026\%$, NS2
285 $0.023 \pm 0.0089\%$). During the FL forest burn experiment, flaming and smoldering phases were
286 not separated for sampling, and the average tNAC_{OM}% is $0.13 \pm 0.059\%$, which is between the
287 tNAC_{OM}% of the flaming and smoldering samples of the NC forest experiments. If we
288 recalculate the average tNAC_{OM}% for the NC forest experiments by combining the flaming and
289 smoldering sample data in each burn, the three BB experiments (FL forest, NC forest 1 and 2)
290 show similar average tNAC_{OM}% (0.11 ± 0.017 – $0.13 \pm 0.059\%$), and the average tNAC_{OM}%
291 across all samples in this work is $0.12 \pm 0.051\%$ (range 0.037 to 0.21%). This value is
292 comparable to that observed at Detling ($\sim 0.5\%$), United Kingdom during winter, when domestic
293 wood burning is prevalent (Mohr et al., 2013). In the current work, most of the NACs were
294 quantified using surrogates, and their contributions to OM from BB may change if authentic
295 standards or different surrogates are used for quantification. However, the three experiments
296 might still have consistent relative mass contribution profiles of NACs and similar average
297 tNAC_{OM}%, assuming burn conditions and fuel types have minor impact on the OM/OC ratio. As
298 shown in Fig. S3e and Fig. 2c, tNAC_{OM}% correlated ($p < 0.05$) with EC/OC for both individual
299 burns and pooled experimental data. Therefore, unlike the light absorption of methanol
300 extractable OC, the formation of NACs in BB seems to depend largely on burn conditions, rather
301 than fuel types and ambient conditions.

302 Among the fourteen identified NAC formulas, C₆H₅NO₄ and C₉H₉NO₄ have the highest
303 concentrations (Fig. 3) in FL forest and NC forest flaming-phase samples, accounting for $0.029 \pm$
304 0.011 to $0.037 \pm 0.011\%$ and 0.023 ± 0.012 to $0.049 \pm 0.016\%$ of the OM, respectively (Table

305 S3). In NC forest smoldering-phase samples, $C_6H_5NO_4$ has the highest mass contribution (NS1
306 $0.024 \pm 0.0098\%$, NS2 $0.010 \pm 0.0027\%$), followed by $C_7H_7NO_4$ (NS1 $0.0087 \pm 0.0030\%$, NS2
307 $0.0043 \pm 0.0010\%$) and $C_9H_9NO_4$ (NS1 $0.0052 \pm 0.0033\%$, NS2 $0.0047 \pm 0.0013\%$) (Table S3).
308 The $C_6H_5NO_4$ was identified as 4-nitrocatechol by comparing its MS/MS spectrum (Fig. 1b) with
309 that of an authentic standard (Fig. S2b) in Xie et al. (2017a). The EIC of $C_9H_9NO_4$ exhibited 3–4
310 isomers (Fig. S1i), while only two MS/MS spectra (Fig. 11,m) were obtained due to the weak
311 EIC intensity for compounds eluting at times ≥ 10 min. The fragmentation patterns of $C_9H_9NO_4$
312 compounds (Fig. 11,m) are different from that of 2,5-dimethyl-4-nitrobenzoic acid (reference
313 standards with the same formula, Fig. S2g) without the loss of CO_2 , suggesting that the $C_9H_9NO_4$
314 compounds identified in this work lack a carboxylic acid group. Both MS/MS spectra of the two
315 $C_9H_9NO_4$ isomers reflect the loss of OCN (Fig. 11,m), suggesting a skeleton of benzoxazole/
316 benzisoxazole or the existence of a cyanate ($-O-C\equiv N$) or isocyanate ($-N=C=O$) group. Volatile
317 organo-isocyanate structures (e.g., CH_3NCO) were identified from anthropogenic biomass
318 burning (Priestley et al., 2018), and benzoxazole structures have been observed in pyrolyzed
319 charcoal smoke (Kaal et al., 2008). Giorgi et al. (2004) investigated the fragmentation of 3-
320 methyl-1,2-benzisoxazole and 2-methyl-1,3-benzoxazole using a CID technique under different
321 energy frames, and found a loss of CO but not OCN for both of them. In this work, four standard
322 compounds, including phenyl cyanate (C_6H_5OCN), benzoxazole (C_7H_5NO), 4-methoxyphenyl
323 isocyanate ($CH_3OC_6H_4NCO$), and 2,4-dimethoxyphenyl isocyanate [$(CH_3O)_2C_6H_3NCO$] were
324 analyzed using a gas chromatography (Agilent 6890) coupled to a mass spectrometer (Agilent
325 5975B) under electron ionization (EI, 70 eV) mode. These compounds do not have a phenol
326 structure and cannot be detected using ESI under negative ion mode. The MS/MS spectra of 4-
327 methoxyphenyl isocyanate and 2,4-dimethoxyphenyl isocyanate were obtained by using a

328 modified method (ESI at positive ion mode) for NACs analysis in this work. As shown in Fig.
329 S4a and b, the loss of OCN is observed for phenyl cyanate, but not benzoxazole. In Fig. S4c and
330 d, the ions at m/z 106 and 136 can be produced from the species at m/z 149 and 179 through the
331 loss of $\text{CH}_3 + \text{CO}$ or $\text{H} + \text{NCO}$ (43 Da). The MS/MS spectra of 4-methoxyphenyl isocyanate and
332 2,4-dimethoxyphenyl isocyanate (Fig. S4e,f) confirmed the loss of $\text{CH}_3 + \text{CO}$, and the loss of
333 CH_3 reflected the presence of methoxy group. As such, the $\text{C}_9\text{H}_9\text{NO}_4$ compounds identified in
334 this work is expected to contain a phenyl cyanate structure.

335 $\text{C}_6\text{H}_5\text{NO}_3$ (Fig. 1a) is identified as 4-nitrophenol using an authentic standard (Fig. S2a).
336 $\text{C}_7\text{H}_7\text{NO}_4$ has at least two isomers as shown in Fig. S1c that are identified as 4-methyl-5-
337 nitrocatechol and 3-methyl-6-nitrocatechol according to Inuma et al. (2010) and Xie et al.
338 (2017a). Referring to the MS/MS spectrum of 4-nitrocatechol (Fig. S2b), the $\text{C}_6\text{H}_5\text{NO}_5$
339 compound should have a nitrocatechol skeleton with an extra hydroxyl group on the benzene
340 ring. Like $\text{C}_9\text{H}_9\text{NO}_4$ (Fig. 1l,m), the loss of OCN was observed for the fragmentation of
341 $\text{C}_8\text{H}_7\text{NO}_4$ in the MS/MS spectra (Fig. 1f,g), and a phenyl cyanate structure was proposed (Table
342 2). However, the fragmentation mechanism associated with the loss of single nitrogen is
343 unknown and warrants further study. The $\text{C}_8\text{H}_9\text{NO}_4$ identified in this work should have several
344 isomers (Fig. S1f), and two representative MS/MS spectra are provided in Fig. 1h and i. The first
345 isomer of $\text{C}_8\text{H}_9\text{NO}_4$ has a dominant ion of m/z 137, reflecting the loss of NO and CH_3 .
346 Comparing to the MS/MS spectrum of 4-nitrophenol (Fig. S2a), the first $\text{C}_8\text{H}_9\text{NO}_4$ isomer might
347 contain a methyl nitrophenol skeleton with a methoxy group. The fragmentation pattern of the
348 second isomer of $\text{C}_8\text{H}_9\text{NO}_4$ is similar as $\text{C}_7\text{H}_7\text{NO}_4$, and the molecule is postulated as ethyl
349 nitrocatechol. $\text{C}_7\text{H}_7\text{NO}_5$ has a similar fragmentation pattern as $\text{C}_6\text{H}_5\text{NO}_4$ and $\text{C}_7\text{H}_7\text{NO}_4$, and is
350 identified as methoxy nitrocatechol. For NC forest burns, $\text{C}_{10}\text{H}_7\text{NO}_3$ was only detected in

351 flaming-phase samples (Fig. 3). The MS/MS spectrum of $C_{10}H_7NO_3$ was subject to considerable
352 noise, although the loss of NO_2 could be identified (Fig. 1k). In Fig. 1n, the ion at m/z 167 is
353 attributed to the loss of two CH_3 from the $[M-H]^-$ ion of $C_8H_9NO_5$, and the loss of $H + CO + NO$
354 is a common feature shared by several nitrophenol-like compounds (Fig. 1b,c,e,i), so the
355 $C_8H_9NO_5$ compound was identified as dimethoxynitrophenol. The MS/MS spectra of $C_{10}H_{11}NO_4$,
356 $C_{10}H_{11}NO_5$, $C_{11}H_{13}NO_5$, and $C_{11}H_{13}NO_6$ were characterized by the loss of CH_3 and/or OCN (Fig.
357 1o–t), indicting the existence of methoxy and/or cyanate groups (Fig. S4). Although the exact
358 structure of these NACs cannot be determined, their functional groups on the benzene ring were
359 proposed in Table 2 from their fragmentation patterns.

360 In this work, three of the identified NACs, 4-nitrophenol, 4-nitrocatechol, and methyl
361 nitrocatechols, were commonly observed in BB emissions or BB impacted atmospheres (Claeys
362 et al., 2014; Mohr et al., 2013; Budisulistiorini et al., 2017). These compounds can also be
363 generated from the photo-oxidation of aromatic VOCs in the presence of NO_x (Iinuma et al.,
364 2010; Lin et al., 2015; Xie et al., 2017a). Both BB and fossil fuel combustion can emit a mixture
365 of aromatic precursors (e.g., benzene, toluene) for secondary NACs formation (Martins et al.,
366 2006; Lewis et al., 2013; George et al., 2014; Gilman et al., 2015; Hatch et al., 2015; George et al.,
367 2015). Therefore, the NACs uniquely related to BB are needed to represent BB emissions. In this
368 work, the NACs formula with molecular weight (MW) < 200 Da (from $C_6H_5NO_3$, 138 Da to
369 $C_8H_9NO_5$, 198 Da) were all identified in secondary organic aerosol (SOA) generated from
370 chamber reactions with NO_x (Xie et al., 2017a). However, the NACs from BB emissions and
371 SOA formations with identical formulas might have different structures. For example, the
372 MS/MS spectra of $C_7H_7NO_5$ and $C_8H_9NO_5$ from BB in this work and aromatic VOCs/ NO_x
373 reactions in Xie et al. (2017a) had distinct fragmentation patterns (Fig. S5). In Xie et al. (2017a),

374 the $C_8H_7NO_4$ and $C_9H_9NO_4$ generated from ethylbenzene/ NO_x reactions might have fragile
375 structures and their MS/MS spectra were not available. In this work, $C_8H_7NO_4$ and $C_9H_9NO_4$
376 from BB emissions are more stable and are supposed to have a phenyl cyanate structure. Among
377 the four NAC formulas with MW > 200 Da identified in this work (Table 2), $C_{10}H_{11}NO_4$ was
378 also observed as 5-methoxy-4-nitro-2-(prop-2-en-1-yl)phenol in SOA from reactions of methyl
379 chavicol and NO_x (Pereira et al. (2015), which cannot be assigned to the $C_{10}H_{11}NO_4$ from BB
380 emissions in this work. Compared to the NACs in aromatic VOCs/ NO_x SOA (Inuma et al., 2010;
381 Lin et al., 2015; Xie et al., 2017a; Pereira et al., 2015), the structures of NACs from BB in this
382 work were characterized by methoxy and cyanate groups. The methoxyphenol structure is a
383 feature in polar organic compounds from BB (Schauer et al., 2001; Simpson et al.,
384 2005; Mazzoleni et al., 2007). The cyanate group was rarely reported in gas- or particle-phase
385 pollutants from BB, which might be a missed feature of BB NACs. Vähäsavo et al. (2015)
386 found that cyanate could be formed during the thermal conversion (e.g., pyrolysis, gasification)
387 of black liquor, which is the waste product from the kraft process when digesting pulpwood into
388 paper pulp and composed by an aqueous solution of mixed biomass residues. According to Table
389 2 and Fig. 3, the NACs containing methoxy and/or cyanate groups are predominately generated
390 during the flaming phase in the two NC forest experiments. Before using these compounds as
391 source markers for BB NACs, additional work is warranted to understand their exact structures
392 and lifetimes in the atmosphere. The quantification of these compounds might also be subject to
393 high variability due to the usage of surrogates.

394 **3.3 Contribution of NACs to Abs_{365} .**

395 For each sample extract, individual NACs contributions to Abs_{365} ($Abs_{365,NAC\%}$) were
396 calculated using their mass concentrations ($ng\ m^{-3}$) and the MAC_{365} values of individual

397 compound standards ($MAC_{365,NAC}$), as applied in Zhang et al. (2013) and Xie et al. (2017a). Here,
398 the $MAC_{365,NAC}$ value is OM based with a unit of $m^2 g^{-1}$. Each NAC formula was assigned to an
399 authentic or surrogate standard compound to estimate the contribution to Abs_{365} of extracted OM
400 (Table 2). Except the NACs with a phenyl cyanate structure, the standard compounds used for
401 the NACs absorption calculation and mass quantification were the same (Table 2), and their UV-
402 Vis spectra were obtained from Xie et al. (2017a) and shown in Fig. S6a. The UV-Vis spectra of
403 three standard compounds with cyanate or isocyanate groups are given in Fig. S6b, and none of
404 them has absorption in the range from 350 to 550 nm. As such, the NACs with cyanate groups
405 identified in this work were supposed to have no contribution to bulk Abs_{365} . Details of the
406 method for $Abs_{365,NAC}\%$ calculation are provided in Xie et al. (2017a) and the $MAC_{365,NAC}$ values
407 for identified NACs formulas in this work are listed in Table S4. Since the standard compounds
408 used in this work have no absorption at 550 nm, the identified NACs contributions to Abs_{550}
409 were expected to be 0. The average and ranges of $Abs_{365,NAC}\%$ in BB samples are listed in Table
410 S5. For simplicity, the average $Abs_{365,NAC}\%$ in the five groups of BB samples (FF, NF1 and 2,
411 NS1 and 2) are stacked in Fig. 4.

412 In general, the average contributions of total NACs to Abs_{365} ($Abs_{365,tNAC}\%$ 0.087 ± 0.024
413 to $1.22 \pm 0.54\%$) were 3–10 times higher than their average $tNAC_{OM}\%$ (0.023 ± 0.0089 to $0.18 \pm$
414 0.067%) in BB samples (Tables S5 and S3), indicating that the identified NACs with
415 contributions to Abs_{365} (not including those with cyanate groups) are strong BrC chromophores.
416 Similar to the NACs mass contributions and compositions, the samples collected during flaming
417 periods (NF1 and NF2) had significantly higher ($p < 0.05$) average $Abs_{365,tNAC}\%$ (NF1 $1.21 \pm$
418 0.38% , NF2 $0.42 \pm 0.15\%$) than those collected during smoldering periods (NS1 $0.72 \pm 0.27\%$,
419 NS2 $0.087 \pm 0.024\%$); $Abs_{365,tNAC}\%$ correlated ($p < 0.05$) with EC/OC for both individual burns

420 (Fig. S3f) and pooled experimental data (Fig. 2d). $C_6H_5NO_4$ (0.037 ± 0.0080 to $0.31 \pm 0.11\%$)
421 and $C_7H_7NO_4$ (0.029 ± 0.0051 to $0.27 \pm 0.12\%$) have the highest $Ab_{S_{365},NAC}\%$ among the
422 identified NACs across all the three BB experiments (Table S5). The average $Ab_{S_{365},NAC}\%$
423 values here are comparable to those obtained for atmospheric particles in Germany (0.10 ± 0.06
424 to $1.13 \pm 1.03\%$) (Teich et al., 2017) and Detling, United Kingdom ($4 \pm 2\%$) (Mohr et al., 2013),
425 but more than 10 times lower than those from chamber reactions of benzene ($28.0 \pm 8.86\%$),
426 naphthalene ($20.3 \pm 8.01\%$) and *m*-cresol ($50.5 \pm 15.8\%$) with NO_x (Xie et al., 2017a). Lin et al.
427 (2016, 2017) calculated the absorbance fraction contributed by NACs in BB OC based on signal
428 peaks at particular retention times in HPLC/photodiode array (PDA) spectrophotometry
429 chromatograms, and attributed a large portion (up to or greater than 50%) of the solvent extracts
430 absorption to a limited number of NACs with MW mostly lower than 500 Da. However, the
431 absorbance signals in HPLC/PDA chromatograms are composed by a mixture of light-absorbing
432 compounds due to coelution, and some of them are not NACs or even cannot be ionized with ESI.
433 In this study, standards or surrogates were used to calculate absorption for individual NACs
434 molecules. These different approaches gave different results. Di Lorenzo et al. (2017) studied the
435 absorbance as a function of molecular size of organic aerosols from BB, and concluded that the
436 majority of aqueous extracts absorption ($\lambda = 300$ nm) was due to compounds with MW greater
437 than 500 Da and carbon number greater than 20. In this work, less than 2% of the BrC absorption
438 in BB aerosols at $\lambda = 365$ was ascribed to the identified NACs with a MW range of 138 to 254
439 Da, of which the contribution at longer wavelength ($\lambda = 550$ nm) was expected to be 0. Future
440 work is needed to identify high MW light-absorbing compounds in BB aerosols to apportion a
441 greater fraction of BrC absorption in BB aerosols.

442 **4 Conclusions**

443 The comparisons of light-absorbing properties (MAC_{365} , MAC_{550} , and \dot{A}_{abs}) of BB OC
444 with EC/OC in this study support that burn conditions are not the only factor impacting BrC
445 absorption. Other factors like fuel type or ambient conditions may also play important roles in
446 determining BrC absorption from BB. It may be impractical to predict BrC absorption solely
447 based on EC/OC ratios in BB emissions from different fuels or over different seasons. The
448 present study identified fourteen NAC chemical formulas in BB aerosols. The average $tNAC_{OM}\%$
449 of the FL forest, NC forest 1 and 2 (flaming and smoldering samples were combined)
450 experiments were $0.13 \pm 0.059\%$, $0.13 \pm 0.067\%$, and $0.11 \pm 0.017\%$ by weight, respectively,
451 and the NAC composition was also similar across the three BB experiments. Most of the NACs
452 formulas identified in this work were also observed in simulated SOA generated from chamber
453 reactions of aromatic VOCs with NO_x , but the same NAC formula from BB and SOA could not
454 be assigned to the identical compound. In this work, the structures of NACs from BB were
455 characterized by methoxy and cyanate groups, which were predominately generated during the
456 flaming phase and might be an important feature for BB NACs. More work is warranted to
457 understand their exact structures and lifetimes. The average $tNAC_{OM}\%$ and $Abs_{365,tNAC}\%$ of the
458 flaming-phase samples were significantly higher ($p < 0.05$) than those of smoldering-phase
459 samples in the two NC forest BB experiments. Unlike the bulk MAC_{365} and MAC_{550} , $tNAC_{OM}\%$
460 and $Abs_{365,tNAC}\%$ correlated ($p < 0.05$) with EC/OC for both individual burns and pooled
461 experimental data, suggesting that burn conditions are an important factor in determining NACs
462 formation in BB. Except the compounds with cyanate groups, the NACs identified in this work
463 are likely strong BrC chromophores, as the average contributions of total NACs to bulk Abs_{365}
464 (0.0087 ± 0.024 to $1.22 \pm 0.54\%$) are 3–10 times higher than their average mass contributions to
465 OM (0.023 ± 0.0089 to $0.18 \pm 0.067\%$). However, more light-absorbing compounds from BB

466 with high MW need to be identified to apportion the unknown fraction (> 98%) of BrC
467 absorption.

468

469

470 **Competing interests**

471 The authors declare that they have no conflict of interest.

472 **Disclaimer**

473 The views expressed in this article are those of the authors and do not necessarily represent the
474 views or policies of the U.S. Environmental Protection Agency.

475 **Author contribution**

476 MX and AH designed the research. MX and XC performed the experiments. AH and MH
477 managed sample collection. MX analyzed the data and wrote the paper with significant
478 contributions from all co-authors.

479 **Acknowledgements**

480 This research was supported by the National Natural Science Foundation of China (NSFC,
481 41701551), the State Key Laboratory of Pollution Control and Resource Reuse Foundation (No.
482 PCRRF17040), and the Startup Foundation for Introducing Talent of NUIST (No.
483 2243141801001). We would like to acknowledge Brian Gullett, Johanna Aurell, and Brannon
484 Seay for assistance with laboratory biomass burning sampling. This work was funded by the U.S.
485 Environmental Protection Agency. Data used in the writing of this manuscript is available at the
486 U.S. Environmental Protection Agency's Environmental Dataset Gateway (<https://edg.epa.gov>).

487

488

489 **References**

- 490 Akagi, S. K., Yokelson, R. J., Wiedinmyer, C., Alvarado, M. J., Reid, J. S., Karl, T., Crouse, J. D., and Wennberg,
491 P. O.: Emission factors for open and domestic biomass burning for use in atmospheric models, *Atmos. Chem.*
492 *Phys.*, 11, 4039-4072, 10.5194/acp-11-4039-2011, 2011.
- 493 Anderson, T. L., Charlson, R. J., Schwartz, S. E., Knutti, R., Boucher, O., Rodhe, H., and Heintzenberg, J.: Climate
494 forcing by aerosols-a hazy picture, *Science*, 300, 1103-1104, 10.1126/science.1084777, 2003.
- 495 Aurell, J., and Gullett, B. K.: Emission factors from aerial and ground measurements of field and laboratory forest
496 burns in the southeastern U.S.: PM_{2.5}, black and brown carbon, VOC, and PCDD/PCDF, *Environ. Sci.*
497 *Technol.*, 47, 8443-8452, 10.1021/es402101k, 2013.
- 498 Aurell, J., Gullett, B. K., and Tabor, D.: Emissions from southeastern U.S. grasslands and pine savannas:
499 comparison of aerial and ground field measurements with laboratory burns, *Atmos. Environ.*, 111, 170-178,
500 <http://dx.doi.org/10.1016/j.atmosenv.2015.03.001>, 2015.
- 501 Bond, T. C.: Spectral dependence of visible light absorption by carbonaceous particles emitted from coal
502 combustion, *Geophys. Res. Lett.*, 28, 4075-4078, 10.1029/2001gl013652, 2001.
- 503 Bond, T. C., Streets, D. G., Yarber, K. F., Nelson, S. M., Woo, J.-H., and Klimont, Z.: A technology-based global
504 inventory of black and organic carbon emissions from combustion, *J. Geophys. Res.*, 109, D14,
505 10.1029/2003jd003697, 2004.
- 506 Bond, T. C., and Bergstrom, R. W.: Light absorption by carbonaceous particles: an investigative review, *Aerosol Sci.*
507 *Tech.*, 40, 27-67, 10.1080/02786820500421521, 2006.
- 508 Bond, T. C., Doherty, S. J., Fahey, D. W., Forster, P. M., Berntsen, T., DeAngelo, B. J., Flanner, M. G., Ghan, S.,
509 Kärcher, B., Koch, D., Kinne, S., Kondo, Y., Quinn, P. K., Sarofim, M. C., Schultz, M. G., Schulz, M.,
510 Venkataraman, C., Zhang, H., Zhang, S., Bellouin, N., Guttikunda, S. K., Hopke, P. K., Jacobson, M. Z., Kaiser,
511 J. W., Klimont, Z., Lohmann, U., Schwarz, J. P., Shindell, D., Storelvmo, T., Warren, S. G., and Zender, C. S.:
512 Bounding the role of black carbon in the climate system: A scientific assessment, *J. Geophys. Res.*, 118, 5380-
513 5552, 10.1002/jgrd.50171, 2013.
- 514 Budisulistiorini, S. H., Riva, M., Williams, M., Chen, J., Itoh, M., Surratt, J. D., and Kuwata, M.: Light-absorbing
515 brown carbon aerosol constituents from combustion of Indonesian peat and biomass, *Environ. Sci. Technol.*, 51,
516 4415-4423, 10.1021/acs.est.7b00397, 2017.
- 517 Chakrabarty, R. K., Gyawali, M., Yatavelli, R. L. N., Pandey, A., Watts, A. C., Knue, J., Chen, L. W. A., Pattison, R.
518 R., Tsibert, A., Samburova, V., and Moosmüller, H.: Brown carbon aerosols from burning of boreal peatlands:
519 microphysical properties, emission factors, and implications for direct radiative forcing, *Atmos. Chem. Phys.*,
520 16, 3033-3040, 10.5194/acp-16-3033-2016, 2016.
- 521 Chakrabarty, R. K., Moosmüller, H., Chen, L. W. A., Lewis, K., Arnott, W. P., Mazzoleni, C., Dubey, M. K., Wold,
522 C. E., Hao, W. M., and Kreidenweis, S. M.: Brown carbon in tar balls from smoldering biomass combustion,
523 *Atmos. Chem. Phys.*, 10, 6363-6370, 10.5194/acp-10-6363-2010, 2010.
- 524 Chen, L., W.A. Doddridge, B. G., Dickerson, R. R., Chow, J. C., Mueller, P. K., Quinn, J., and Butler, W. A.:
525 Seasonal variations in elemental carbon aerosol, carbon monoxide and sulfur dioxide: Implications for sources,
526 *Geophys. Res. Lett.*, 28, 1711-1714, 10.1029/2000gl012354, 2001.
- 527 Chen, Y., Sheng, G., Bi, X., Feng, Y., Mai, B., and Fu, J.: Emission factors for carbonaceous particles and
528 polycyclic aromatic hydrocarbons from residential coal combustion in China, *Environ. Sci. Technol.*, 39, 1861-
529 1867, 10.1021/es0493650, 2005.
- 530 Chen, Y., and Bond, T. C.: Light absorption by organic carbon from wood combustion, *Atmos. Chem. Phys.*, 10,
531 1773-1787, 10.5194/acp-10-1773-2010, 2010.
- 532 Chow, K. S., Huang, X. H. H., and Yu, J. Z.: Quantification of nitroaromatic compounds in atmospheric fine
533 particulate matter in Hong Kong over 3 years: field measurement evidence for secondary formation derived
534 from biomass burning emissions, *Environ. Chem.*, 13, 665-673, <https://doi.org/10.1071/EN15174>, 2016.
- 535 Chung, S. H., and Seinfeld, J. H.: Global distribution and climate forcing of carbonaceous aerosols, *J. Geophys. Res.*,
536 107, AAC 14-11-AAC 14-33, 10.1029/2001jd001397, 2002.
- 537 Claeys, M., Vermeylen, R., Yasmeen, F., Gómez-González, Y., Chi, X., Maenhaut, W., Mészáros, T., and Salma, I.:
538 Chemical characterisation of humic-like substances from urban, rural and tropical biomass burning
539 environments using liquid chromatography with UV/vis photodiode array detection and electrospray ionisation
540 mass spectrometry, *Environ. Chem.*, 9, 273-284, <https://doi.org/10.1071/EN11163>, 2012.

541 Desyaterik, Y., Sun, Y., Shen, X., Lee, T., Wang, X., Wang, T., and Collett, J. L.: Speciation of “brown” carbon in
542 cloud water impacted by agricultural biomass burning in eastern China, *J. Geophys. Res.*, 118, 7389-7399,
543 10.1002/jgrd.50561, 2013.

544 Di Lorenzo, R. A., Washenfelder, R. A., Attwood, A. R., Guo, H., Xu, L., Ng, N. L., Weber, R. J., Baumann, K.,
545 Edgerton, E., and Young, C. J.: Molecular-size-separated brown carbon absorption for biomass-burning aerosol
546 at multiple field sites, *Environ. Sci. Technol.*, 51, 3128-3137, 10.1021/acs.est.6b06160, 2017.

547 Eriksson, A., Nordin, E., Nystrom, R., Pettersson, E., Swietlicki, E., Bergvall, C., Westerholm, R., Boman, C., and
548 Pagels, J.: Particulate PAH emissions from residential biomass combustion: time-resolved analysis with aerosol
549 mass spectrometry, *Environ. Sci. Technol.*, 48, 7143-7150, 10.1021/es500486j, 2014.

550 George, I. J., Hays, M. D., Snow, R., Faircloth, J., George, B. J., Long, T., and Baldauf, R. W.: Cold temperature
551 and biodiesel fuel effects on speciated emissions of volatile organic compounds from diesel trucks, *Environ. Sci.*
552 *Technol.*, 48, 14782-14789, 10.1021/es502949a, 2014.

553 George, I. J., Hays, M. D., Herrington, J. S., Preston, W., Snow, R., Faircloth, J., George, B. J., Long, T., and
554 Baldauf, R. W.: Effects of cold temperature and ethanol content on VOC emissions from light-duty gasoline
555 vehicles, *Environ. Sci. Technol.*, 49, 13067-13074, 10.1021/acs.est.5b04102, 2015.

556 Gilman, J. B., Lerner, B. M., Kuster, W. C., Goldan, P. D., Warneke, C., Veres, P. R., Roberts, J. M., de Gouw, J. A.,
557 Burling, I. R., and Yokelson, R. J.: Biomass burning emissions and potential air quality impacts of volatile
558 organic compounds and other trace gases from fuels common in the US, *Atmos. Chem. Phys.*, 15, 13915-13938,
559 10.5194/acp-15-13915-2015, 2015.

560 Giorgi, G., Salvini, L., and Ponticelli, F.: Gas phase ion chemistry of the heterocyclic isomers 3-methyl-1,2-
561 benzisoxazole and 2-methyl-1,3-benzoxazole, *J. Am. Soc. Mass Spectrom.*, 15, 1005-1013,
562 <https://doi.org/10.1016/j.jasms.2004.04.002>, 2004.

563 Grandesso, E., Gullett, B., Touati, A., and Tabor, D.: Effect of moisture, charge size, and chlorine concentration on
564 PCDD/F emissions from simulated open burning of forest biomass, *Environ. Sci. Technol.*, 45, 3887-3894,
565 10.1021/es103686t, 2011.

566 Hatch, L. E., Luo, W., Pankow, J. F., Yokelson, R. J., Stockwell, C. E., and Barsanti, K.: Identification and
567 quantification of gaseous organic compounds emitted from biomass burning using two-dimensional gas
568 chromatography–time-of-flight mass spectrometry, *Atmos. Chem. Phys.*, 15, 1865-1899, 10.5194/acp-15-1865-
569 2015, 2015.

570 Hecobian, A., Zhang, X., Zheng, M., Frank, N., Edgerton, E. S., and Weber, R. J.: Water-soluble organic aerosol
571 material and the light-absorption characteristics of aqueous extracts measured over the Southeastern United
572 States, *Atmos. Chem. Phys.*, 10, 5965-5977, 10.5194/acp-10-5965-2010, 2010.

573 Holder, A. L., Hagler, G. S. W., Aurell, J., Hays, M. D., and Gullett, B. K.: Particulate matter and black carbon
574 optical properties and emission factors from prescribed fires in the southeastern United States, *J. Geophys. Res.*,
575 121, 3465-3483, 10.1002/2015jd024321, 2016.

576 Hosseini, S., Urbanski, S., Dixit, P., Qi, L., Burling, I. R., Yokelson, R. J., Johnson, T. J., Shrivastava, M., Jung, H.,
577 and Weise, D. R.: Laboratory characterization of PM emissions from combustion of wildland biomass fuels, *J.*
578 *Geophys. Res.*, 118, 9914-9929, 10.1002/jgrd.50481, 2013.

579 Huang, R.-J., Yang, L., Cao, J., Chen, Y., Chen, Q., Li, Y., Duan, J., Zhu, C., Dai, W., Wang, K., Lin, C., Ni, H.,
580 Corbin, J. C., Wu, Y., Zhang, R., Tie, X., Hoffmann, T., O’Dowd, C., and Dusek, U.: Brown carbon aerosol in
581 urban Xi’an, Northwest China: the composition and light absorption properties, *Environ. Sci. Technol.*, 52,
582 6825-6833, 10.1021/acs.est.8b02386, 2018.

583 Iinuma, Y., Böge, O., Gräfe, R., and Herrmann, H.: Methyl-nitrocatechols: atmospheric tracer compounds for
584 biomass burning secondary organic aerosols, *Environ. Sci. Technol.*, 44, 8453-8459, 10.1021/es102938a, 2010.

585 Kaal, J., Martínez Cortizas, A., and Nierop, K. G. J.: Characterisation of aged charcoal using a coil probe pyrolysis-
586 GC/MS method optimised for black carbon, *J. Anal. Appl. Pyrol.*, 85, 408-416,
587 <https://doi.org/10.1016/j.jaap.2008.11.007>, 2009.

588 Kirchstetter, T. W., Novakov, T., and Hobbs, P. V.: Evidence that the spectral dependence of light absorption by
589 aerosols is affected by organic carbon, *J. Geophys. Res.*, 109, D21208, 10.1029/2004jd004999, 2004.

590 Lack, D. A., and Langridge, J. M.: On the attribution of black and brown carbon light absorption using the
591 Ångström exponent, *Atmos. Chem. Phys.*, 13, 10535-10543, 10.5194/acp-13-10535-2013, 2013.

592 Laskin, A., Laskin, J., and Nizkorodov, S. A.: Chemistry of atmospheric brown carbon, *Chem. Rev.*, 115, 4335-
593 4382, 10.1021/cr5006167, 2015.

594 Lewis, A. C., Evans, M. J., Hopkins, J. R., Punjabi, S., Read, K. A., Purvis, R. M., Andrews, S. J., Moller, S. J.,
595 Carpenter, L. J., Lee, J. D., Rickard, A. R., Palmer, P. I., and Parrington, M.: The influence of biomass burning
596 on the global distribution of selected non-methane organic compounds, *Atmos. Chem. Phys.*, 13, 851-867,
597 10.5194/acp-13-851-2013, 2013.

598 Lin, P., Liu, J. M., Shilling, J. E., Kathmann, S. M., Laskin, J., and Laskin, A.: Molecular characterization of brown
599 carbon (BrC) chromophores in secondary organic aerosol generated from photo-oxidation of toluene, *Phys.*
600 *Chem. Chem. Phys.*, 17, 23312-23325, 10.1039/c5cp02563j, 2015.

601 Lin, P., Aiona, P. K., Li, Y., Shiraiwa, M., Laskin, J., Nizkorodov, S. A., and Laskin, A.: Molecular characterization
602 of brown carbon in biomass burning aerosol particles, *Environ. Sci. Technol.*, 50, 11815-11824,
603 10.1021/acs.est.6b03024, 2016.

604 Lin, P., Bluvshstein, N., Rudich, Y., Nizkorodov, S. A., Laskin, J., and Laskin, A.: Molecular chemistry of
605 atmospheric brown carbon inferred from a nationwide biomass burning event, *Environ. Sci. Technol.*, 51,
606 11561-11570, 10.1021/acs.est.7b02276, 2017.

607 Lin, Y.-H., Budisulistiorini, S. H., Chu, K., Siejack, R. A., Zhang, H., Riva, M., Zhang, Z., Gold, A., Kautzman, K.
608 E., and Surratt, J. D.: Light-absorbing oligomer formation in secondary organic aerosol from reactive uptake of
609 isoprene epoxydiols, *Environ. Sci. Technol.*, 48, 12012-12021, 10.1021/es503142b, 2014.

610 Lu, Z., Streets, D. G., Winijkul, E., Yan, F., Chen, Y., Bond, T. C., Feng, Y., Dubey, M. K., Liu, S., Pinto, J. P., and
611 Carmichael, G. R.: Light absorption properties and radiative effects of primary organic aerosol emissions,
612 *Environ. Sci. Technol.*, 49, 4868-4877, 10.1021/acs.est.5b00211, 2015.

613 Martins, L. D., Andrade, M. F., Freitas, E. D., Preto, A., Gatti, L. V., Albuquerque, É. L., Tomaz, E., Guardani, M.
614 L., Martins, M. H. R. B., and Junior, O. M. A.: Emission factors for gas-powered vehicles traveling through
615 road tunnels in São Paulo, Brazil, *Environ. Sci. Technol.*, 40, 6722-6729, 10.1021/es052441u, 2006.

616 Martinsson, J., Eriksson, A., Nielsen, I. E., Malmborg, V. B., Ahlberg, E., Andersen, C., Lindgren, R., Nystrom, R.,
617 Nordin, E., and Brune, W.: Impacts of combustion conditions and photochemical processing on the light
618 absorption of biomass combustion aerosol, *Environ. Sci. Technol.*, 49, 14663-14671, 10.1021/acs.est.5b03205,
619 2015.

620 Mazzoleni, L. R., Zielinska, B., and Moosmüller, H.: Emissions of levoglucosan, methoxy phenols, and organic
621 acids from prescribed burns, laboratory combustion of wildland fuels, and residential wood combustion,
622 *Environ. Sci. Technol.*, 41, 2115-2122, 10.1021/es061702c, 2007.

623 McMeeking, G., Fortner, E., Onasch, T., Taylor, J., Flynn, M., Coe, H., and Kreidenweis, S.: Impacts of
624 nonrefractory material on light absorption by aerosols emitted from biomass burning, *J. Geophys. Res.*, 119,
625 12,272-212,286, 2014.

626 Mohr, C., Lopez-Hilfiker, F. D., Zotter, P., Prévôt, A. S. H., Xu, L., Ng, N. L., Herndon, S. C., Williams, L. R.,
627 Franklin, J. P., Zahniser, M. S., Worsnop, D. R., Knighton, W. B., Aiken, A. C., Gorkowski, K. J., Dubey, M.
628 K., Allan, J. D., and Thornton, J. A.: Contribution of nitrated phenols to wood burning brown carbon light
629 absorption in Detling, United Kingdom during winter time, *Environ. Sci. Technol.*, 47, 6316-6324,
630 10.1021/es400683v, 2013.

631 Myhre, G., Samset, B. H., Schulz, M., Balkanski, Y., Bauer, S., Bernsten, T. K., Bian, H., Bellouin, N., Chin, M.,
632 Diehl, T., Easter, R. C., Feichter, J., Ghan, S. J., Hauglustaine, D., Iversen, T., Kinne, S., Kirkevåg, A.,
633 Lamarque, J. F., Lin, G., Liu, X., Lund, M. T., Luo, G., Ma, X., van Noije, T., Penner, J. E., Rasch, P. J., Ruiz,
634 A., Seland, Ø., Skeie, R. B., Stier, P., Takemura, T., Tsigaridis, K., Wang, P., Wang, Z., Xu, L., Yu, H., Yu, F.,
635 Yoon, J. H., Zhang, K., Zhang, H., and Zhou, C.: Radiative forcing of the direct aerosol effect from AeroCom
636 Phase II simulations, *Atmos. Chem. Phys.*, 13, 1853-1877, 10.5194/acp-13-1853-2013, 2013.

637 Nielsen, I. E., Eriksson, A. C., Lindgren, R., Martinsson, J., Nyström, R., Nordin, E. Z., Sadiktsis, I., Boman, C.,
638 Nøjgaard, J. K., and Pagels, J.: Time-resolved analysis of particle emissions from residential biomass
639 combustion—Emissions of refractory black carbon, PAHs and organic tracers, *Atmos. Environ.*, 165, 179-190,
640 2017.

641 NIOSH, 1999. National Institute of Occupational Safety and Health. Elemental carbon (diesel particulate): Method
642 5040, Rep. <https://www.cdc.gov/niosh/docs/2003-154/pdfs/5040f3.pdf> (1999). Accessed March, 2018.

643 Pereira, K. L., Hamilton, J. F., Rickard, A. R., Bloss, W. J., Alam, M. S., Camredon, M., Ward, M. W., Wyche, K.
644 P., Muñoz, A., Vera, T., Vázquez, M., Borrás, E., and Ródenas, M.: Insights into the formation and evolution of
645 individual compounds in the particulate phase during aromatic photo-oxidation, *Environ. Sci. Technol.*, 49,
646 13168-13178, 10.1021/acs.est.5b03377, 2015.

647 Pokhrel, R. P., Wagner, N. L., Langridge, J. M., Lack, D. A., Jayarathne, T., Stone, E. A., Stockwell, C. E.,
648 Yokelson, R. J., and Murphy, S. M.: Parameterization of single-scattering albedo (SSA) and absorption
649 Ångström exponent (AAE) with EC / OC for aerosol emissions from biomass burning, *Atmos. Chem. Phys.*, 16,
650 9549-9561, 10.5194/acp-16-9549-2016, 2016.

651 Priestley, M., Le Breton, M., Bannan, T. J., Leather, K. E., Bacak, A., Reyes-Villegas, E., De Vocht, F., Shallcross,
652 B. M. A., Brazier, T., Anwar Khan, M., Allan, J., Shallcross, D. E., Coe, H., and Percival, C. J.: Observations of
653 isocyanate, amide, nitrate, and nitro compounds from an anthropogenic biomass burning event using a ToF-
654 CIMS, *J. Geophys. Res.*, 123, 7687-7704, doi:10.1002/2017JD027316, 2018.

655 Ramanathan, V., Crutzen, P. J., Kiehl, J. T., and Rosenfeld, D.: Aerosols, climate, and the hydrological cycle,
656 *Science*, 294, 2119-2124, 10.1126/science.1064034, 2001.

657 Reff, A., Bhave, P. V., Simon, H., Pace, T. G., Pouliot, G. A., Mobley, J. D., and Houyoux, M.: Emissions inventory
658 of PM_{2.5} trace elements across the United States, *Environ. Sci. Technol.*, 43, 5790-5796, 10.1021/es802930x,
659 2009.

660 Riddle, S. G., Jakober, C. A., Robert, M. A., Cahill, T. M., Charles, M. J., and Kleeman, M. J.: Large PAHs detected
661 in fine particulate matter emitted from light-duty gasoline vehicles, *Atmos. Environ.*, 41, 8658-8668,
662 <https://doi.org/10.1016/j.atmosenv.2007.07.023>, 2007.

663 Saleh, R., Robinson, E. S., Tkacik, D. S., Ahern, A. T., Liu, S., Aiken, A. C., Sullivan, R. C., Presto, A. A., Dubey,
664 M. K., Yokelson, R. J., Donahue, N. M., and Robinson, A. L.: Brownness of organics in aerosols from biomass
665 burning linked to their black carbon content, *Nature Geosci.*, 7, 647-650, 10.1038/ngeo2220, 2014.

666 Samburova, V., Connolly, J., Gyawali, M., Yatavelli, R. L. N., Watts, A. C., Chakrabarty, R. K., Zielinska, B.,
667 Moosmüller, H., and Khlystov, A.: Polycyclic aromatic hydrocarbons in biomass-burning emissions and their
668 contribution to light absorption and aerosol toxicity, *Sci. Total Environ.*, 568, 391-401,
669 <http://doi.org/10.1016/j.scitotenv.2016.06.026>, 2016.

670 Schauer, J. J., Kleeman, M. J., Cass, G. R., and Simoneit, B. R. T.: Measurement of emissions from air pollution
671 sources. 3. C1-C29 organic compounds from fireplace combustion of wood, *Environ. Sci. Technol.*, 35, 1716-
672 1728, 10.1021/es001331e, 2001.

673 Simpson, C. D., Paulsen, M., Dills, R. L., Liu, L. J. S., and Kalman, D. A.: Determination of methoxyphenols in
674 ambient atmospheric particulate matter: tracers for wood combustion, *Environ. Sci. Technol.*, 39, 631-637,
675 10.1021/es0486871, 2005.

676 Teich, M., van Pinxteren, D., Kecorius, S., Wang, Z., and Herrmann, H.: First quantification of imidazoles in
677 ambient aerosol particles: potential photosensitizers, brown carbon constituents, and hazardous components,
678 *Environ. Sci. Technol.*, 50, 1166-1173, 10.1021/acs.est.5b05474, 2016.

679 Teich, M., van Pinxteren, D., Wang, M., Kecorius, S., Wang, Z., Müller, T., Močnik, G., and Herrmann, H.:
680 Contributions of nitrated aromatic compounds to the light absorption of water-soluble and particulate brown
681 carbon in different atmospheric environments in Germany and China, *Atmos. Chem. Phys.*, 17, 1653-1672,
682 10.5194/acp-17-1653-2017, 2017.

683 Vähä-Savo, N., DeMartini, N., Engblom, M., Brink, A., and Hupa, M.: The fate of char nitrogen in black liquor
684 combustion—Cyanate formation and decomposition, *Ind. Eng. Chem. Res.*, 54, 2831-2842, 10.1021/ie503450r,
685 2015.

686 Xie, M., Chen, X., Hays, M. D., Lewandowski, M., Offenberg, J., Kleindienst, T. E., and Holder, A. L.: Light
687 absorption of secondary organic aerosol: composition and contribution of nitroaromatic compounds, *Environ.*
688 *Sci. Technol.*, 51, 11607-11616, 10.1021/acs.est.7b03263, 2017a.

689 Xie, M., Hays, M. D., and Holder, A. L.: Light-absorbing organic carbon from prescribed and laboratory biomass
690 burning and gasoline vehicle emissions, *Sci. Rep.*, 7, 7318, 10.1038/s41598-017-06981-8, 2017b.

691 Zhang, X., Lin, Y.-H., Surratt, J. D., and Weber, R. J.: Sources, composition and absorption Ångström exponent of
692 light-absorbing organic components in aerosol extracts from the Los Angeles Basin, *Environ. Sci. Technol.*, 47,
693 3685-3693, 10.1021/es305047b, 2013.

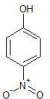
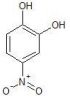
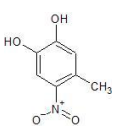
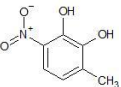
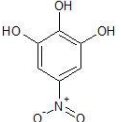
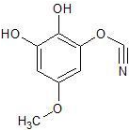
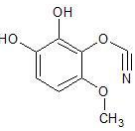
Zhou, Y., Xing, X., Lang, J., Chen, D., Cheng, S., Wei, L., Wei, X., and Liu, C.: A comprehensive biomass burning
emission inventory with high spatial and temporal resolution in China, *Atmos. Chem. Phys.*, 17, 2839-2864,
10.5194/acp-17-2839-2017, 2017.

Table 1. EC/OC ratio, OC extraction efficiency and light-absorbing properties of organic aerosols in PM_{2.5} from laboratory biomass burning.

Experiment	Phase	Abbr.	Fuels	EC/OC	Extraction efficiency (%)	MAC ₃₆₅ (m ² gC ⁻¹)	MAC ₅₅₀ (m ² gC ⁻¹)	Åabs
FL forest ^a	No separation	FF	long leaf pine (N=9)	0.21 ± 0.16	97.0 ± 1.87	1.13 ± 0.15	0.053 ± 0.023	7.36 ± 0.59
NC forest 1	Flaming	NF1	hardwood/loblolly pine (N=3)	0.042 ± 0.014	97.7 ± 0.41	1.47 ± 0.25	0.15 ± 0.065	5.68 ± 0.70
	Smoldering	NS1	hardwood/loblolly pine (N=3)	0.0098 ± 0.0024	97.9 ± 0.22	1.00 ± 0.11	0.054 ± 0.015	6.83 ± 0.52
NC forest 2	Flaming	NF2	hardwood/loblolly pine (4)	0.049 ± 0.011	99.5 ± 0.33	4.07 ± 0.15	0.17 ± 0.0051	7.38 ± 0.069
	Smoldering	NS2	hardwood/loblolly pine (4)	0.0075 ± 0.0026	99.2 ± 0.10	3.25 ± 0.35	0.12 ± 0.033	7.95 ± 0.22

^a Data were obtained from Xie et al. (2017b).

Table 2. Identified N-containing aromatic compounds by HPLC/ESI-Q-ToFMS from laboratory biomass burning in this study.

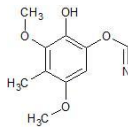
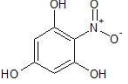
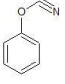
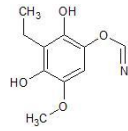
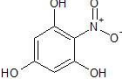
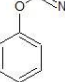
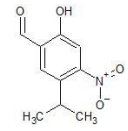
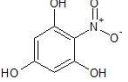
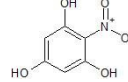
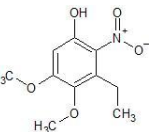
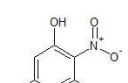
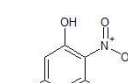
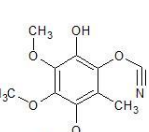
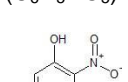
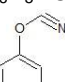
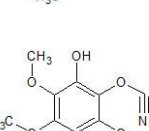
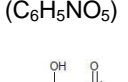
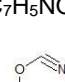
Suggested Formula	Theoretical m/z [M-H] ⁻	Measured m/z [M-H] ⁻	Proposed structure	Quantified as ^b	Absorbing as ^c
C ₆ H ₅ NO ₃	138.0196	138.0198		4-Nitrophenol (C ₆ H ₅ NO ₃)	4-Nitrophenol (C ₆ H ₅ NO ₃)
C ₆ H ₅ NO ₄	154.0145	154.0143		4-Nitrocatechol (C ₆ H ₅ NO ₄)	4-Nitrocatechol (C ₆ H ₅ NO ₄)
C ₇ H ₇ NO ₄ (Iso1 ^a)	168.0302	168.0295		2-Methyl-4-nitroresorcinol (C ₇ H ₇ NO ₄)	2-Methyl-4-nitroresorcinol (C ₇ H ₇ NO ₄)
C ₇ H ₇ NO ₄ (Iso2)	168.0302	168.0291		2-Methyl-4-nitroresorcinol (C ₇ H ₇ NO ₄)	2-Methyl-4-nitroresorcinol (C ₇ H ₇ NO ₄)
C ₆ H ₅ NO ₅	170.0095	170.0087		2-Nitrophenol (C ₆ H ₅ NO ₅)	2-Nitrophenol (C ₆ H ₅ NO ₅)
C ₈ H ₇ NO ₄ (Iso1)	180.0302	180.0305		2-Methyl-5-nitrobenzoic acid (C ₈ H ₇ NO ₄)	phenyl cyanate (C ₇ H ₅ NO)
C ₈ H ₇ NO ₄ (Iso2)	180.0302	180.0290		2-Methyl-5-nitrobenzoic acid (C ₈ H ₇ NO ₄)	phenyl cyanate (C ₇ H ₅ NO)

^a Isomer 1; ^b standard compounds used for the quantification of identified N-containing aromatic compounds; ^c standard compounds used to estimate the light absorption of N-containing aromatic compounds.

Table 2. Continue.

Suggested Formula	Theoretical m/z [M-H] ⁻	Measured m/z [M-H] ⁻	Proposed structure	Quantified as	Absorbing as
C ₈ H ₉ NO ₄ (Iso1)	182.0459	182.0467		 2-Methyl-4-nitroresorcinol (C ₇ H ₇ NO ₄)	 2-Methyl-4-nitroresorcinol (C ₇ H ₇ NO ₄)
C ₈ H ₉ NO ₄ (Iso2)	182.0459	182.0452		 2-Methyl-4-nitroresorcinol (C ₇ H ₇ NO ₄)	 2-Methyl-4-nitroresorcinol (C ₇ H ₇ NO ₄)
C ₇ H ₇ NO ₅	184.0253	184.0259		 2-Nitrophenol (C ₆ H ₅ NO ₅)	 2-Nitrophenol (C ₆ H ₅ NO ₅)
C ₁₀ H ₇ NO ₃	188.0353	188.0356		 2-Nitro-1-naphthol (C ₁₀ H ₇ NO ₃)	 2-Nitro-1-naphthol (C ₁₀ H ₇ NO ₃)
C ₉ H ₉ NO ₄ (Iso1)	194.0458	194.0461		 2,5-Dimethyl-4-nitrobenzoic acid (C ₉ H ₉ NO ₄)	 phenyl cyanate (C ₇ H ₅ NO)
C ₉ H ₉ NO ₄ (Iso2)	194.0458	194.0461		 2,5-Dimethyl-4-nitrobenzoic acid (C ₉ H ₉ NO ₄)	 phenyl cyanate (C ₇ H ₅ NO)
C ₈ H ₉ NO ₅	198.0407	198.0407		 2-Nitrophenol (C ₆ H ₅ NO ₅)	 2-Nitrophenol (C ₆ H ₅ NO ₅)

Table 2. Continue

Suggested Formula	Theoretical m/z [M-H] ⁻	Measured m/z [M-H] ⁻	Proposed structure	Quantified as	Absorbing as
C ₁₀ H ₁₁ NO ₄ (Iso1)	208.0615	208.0621		 2-Nitrofloriglucinol (C ₆ H ₅ NO ₅)	 phenyl cyanate (C ₇ H ₅ NO)
C ₁₀ H ₁₁ NO ₄ (Iso2)	208.0615	208.0607		 2-Nitrofloriglucinol (C ₆ H ₅ NO ₅)	 phenyl cyanate (C ₇ H ₅ NO)
C ₁₀ H ₁₁ NO ₄ (Iso3)	208.0615	208.0616		 2-Nitrofloriglucinol (C ₆ H ₅ NO ₅)	 2-Nitrofloriglucinol (C ₆ H ₅ NO ₅)
C ₁₀ H ₁₁ NO ₅	224.0564	224.0565		 2-Nitrofloriglucinol (C ₆ H ₅ NO ₅)	 2-Nitrofloriglucinol (C ₆ H ₅ NO ₅)
C ₁₁ H ₁₃ NO ₅	238.0721	238.0722		 2-Nitrofloriglucinol (C ₆ H ₅ NO ₅)	 phenyl cyanate (C ₇ H ₅ NO)
C ₁₁ H ₁₃ NO ₆	254.0670	254.0670		 2-Nitrofloriglucinol (C ₆ H ₅ NO ₅)	 phenyl cyanate (C ₇ H ₅ NO)

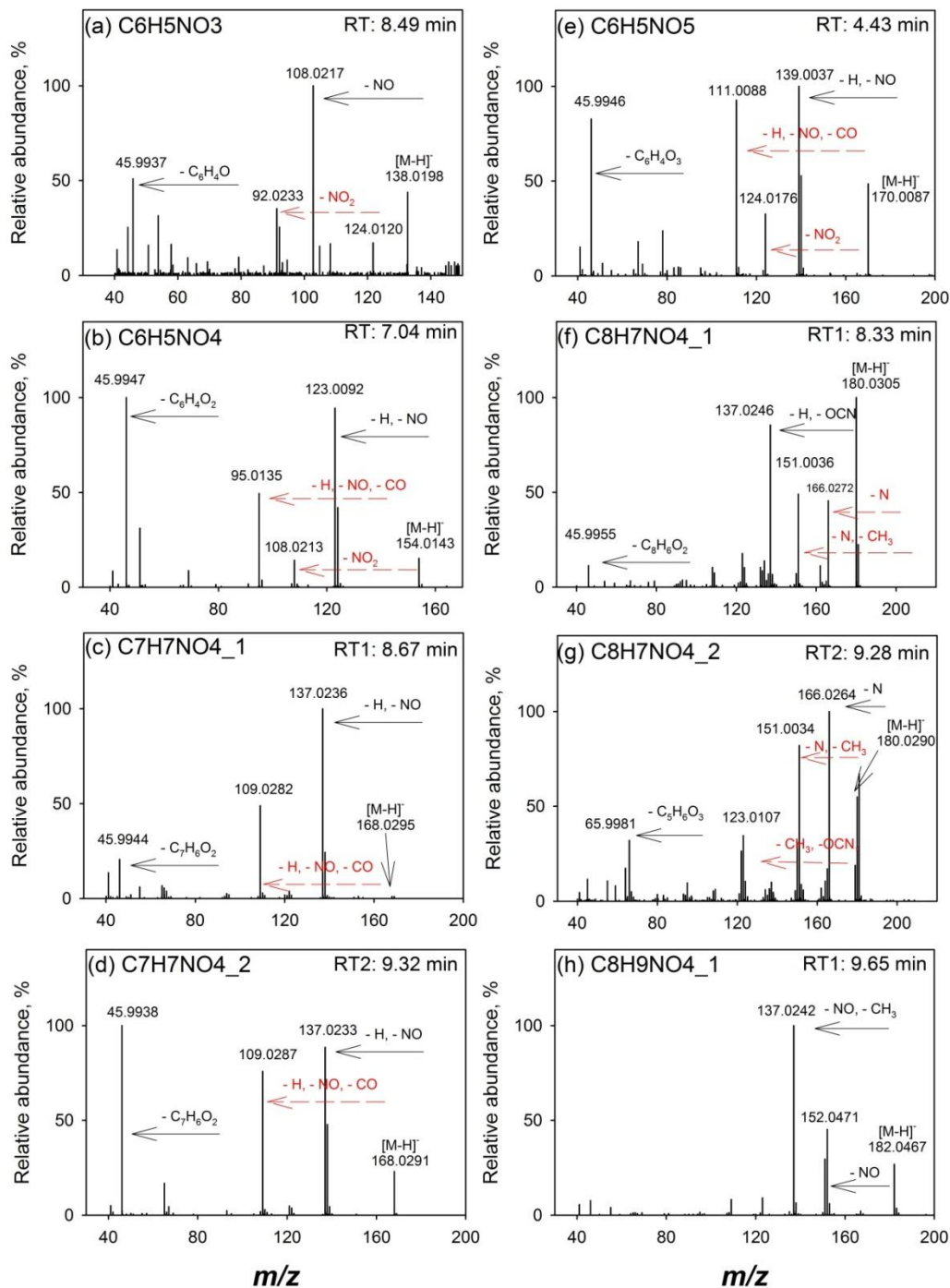


Figure 1. Q-ToF MS/MS spectra of (a) $C_6H_5NO_3$, (b) $C_6H_5NO_4$, (c, d) $C_7H_7NO_4$ isomers (e) $C_6H_5NO_5$, (f, g) $C_8H_7NO_4$ isomers, (h, i) $C_8H_9NO_4$ isomers, (j) $C_7H_7NO_5$, (k) $C_{10}H_7NO_3$, (l, m) $C_9H_9NO_4$ isomers, (n) $C_8H_9NO_5$, (o-q) $C_{10}H_{11}NO_4$ isomers, (r) $C_{10}H_{11}NO_5$, (s) $C_{11}H_{13}NO_5$ and (t) $C_{11}H_{13}NO_6$ identified in the flaming phase sample collected during NC forest 1 experiment, burn 2 (Table S1).

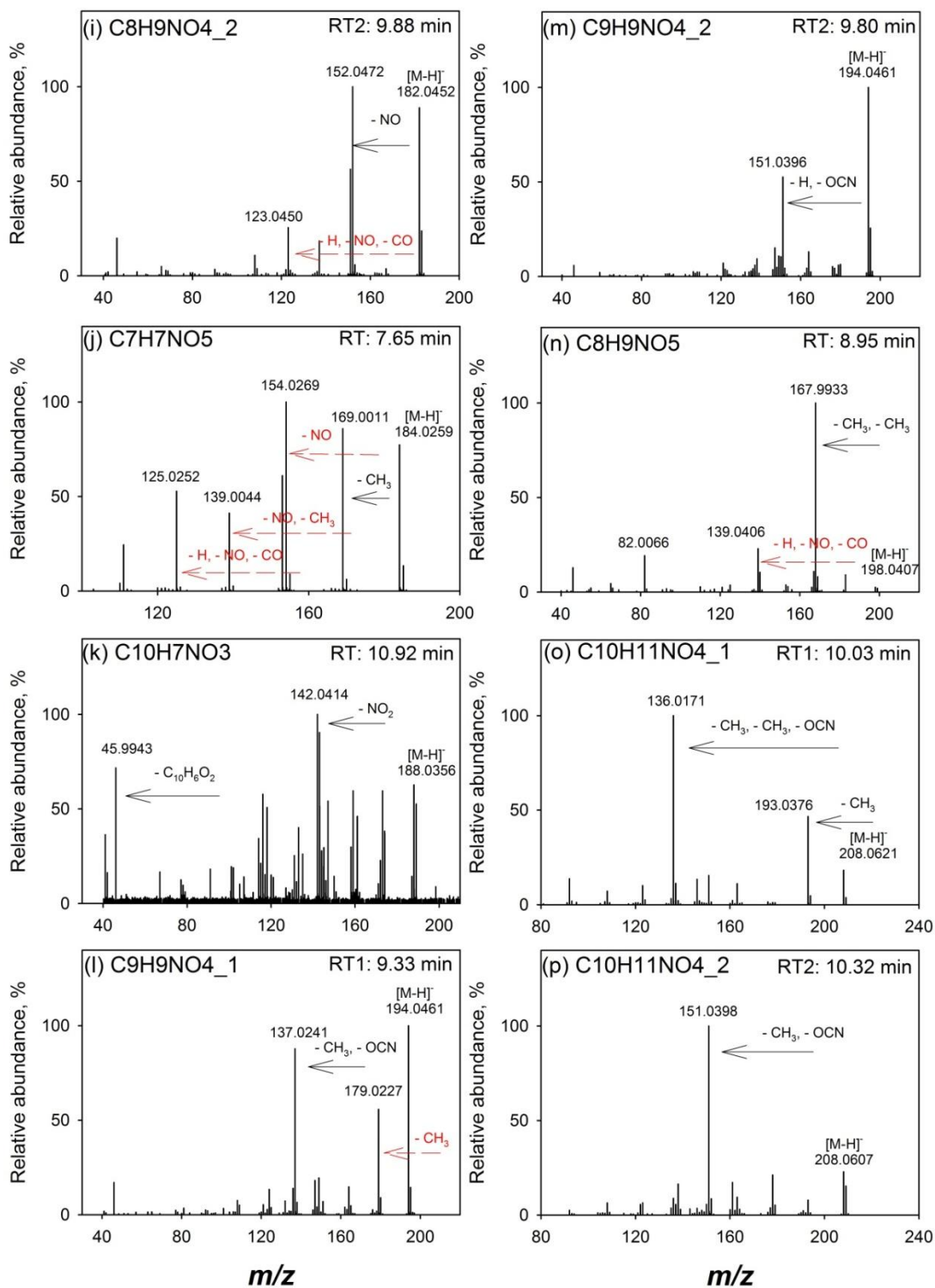


Figure 1. Continue

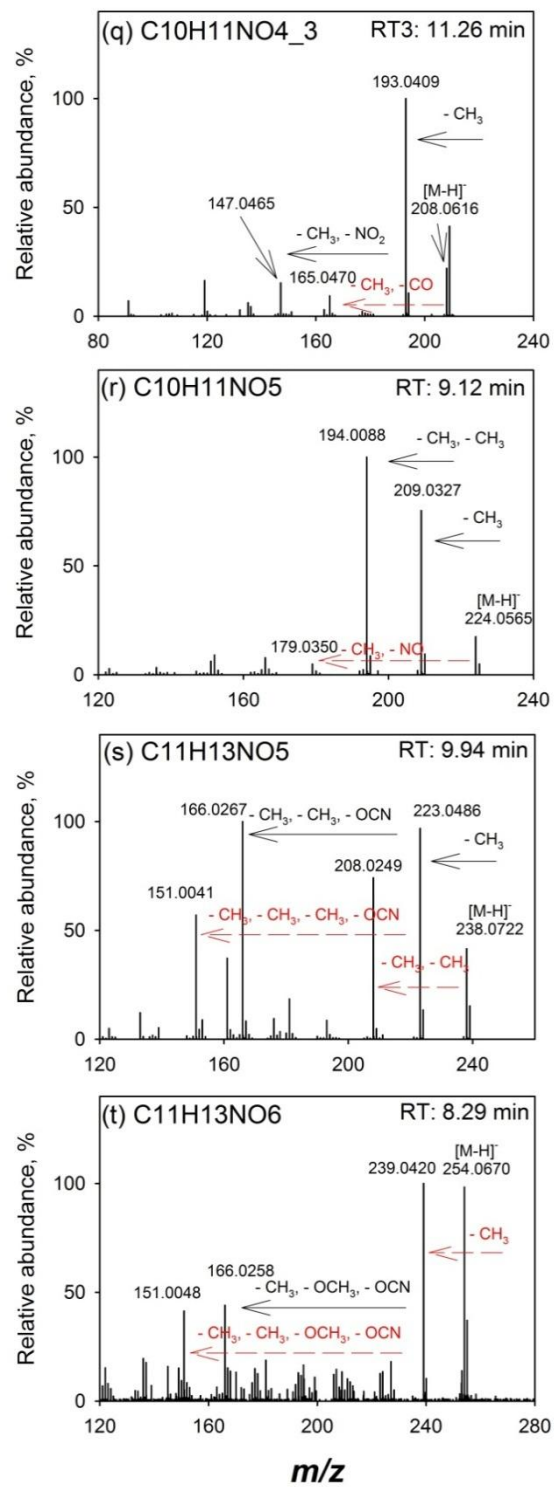


Figure 1. Continue

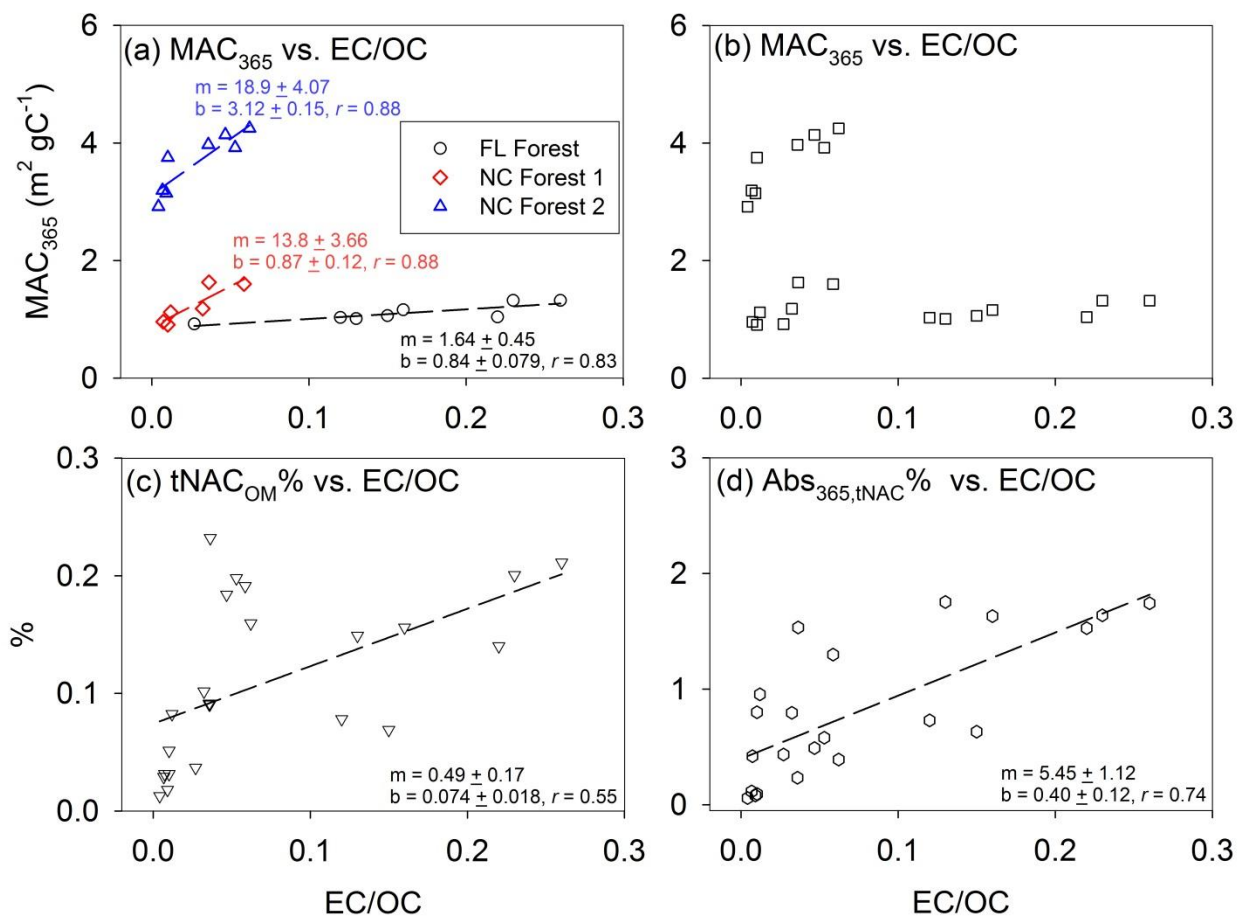


Figure 2. Linear regressions of (a) MAC_{365} vs. EC/OC with individual burns data, (b) MAC_{365} vs. EC/OC, (c) $tNAC_{OM}\%$ vs. EC/OC and (d) $Abs_{365,tNAC}\%$ vs. EC/OC with pooled measurements of all the three experiments.

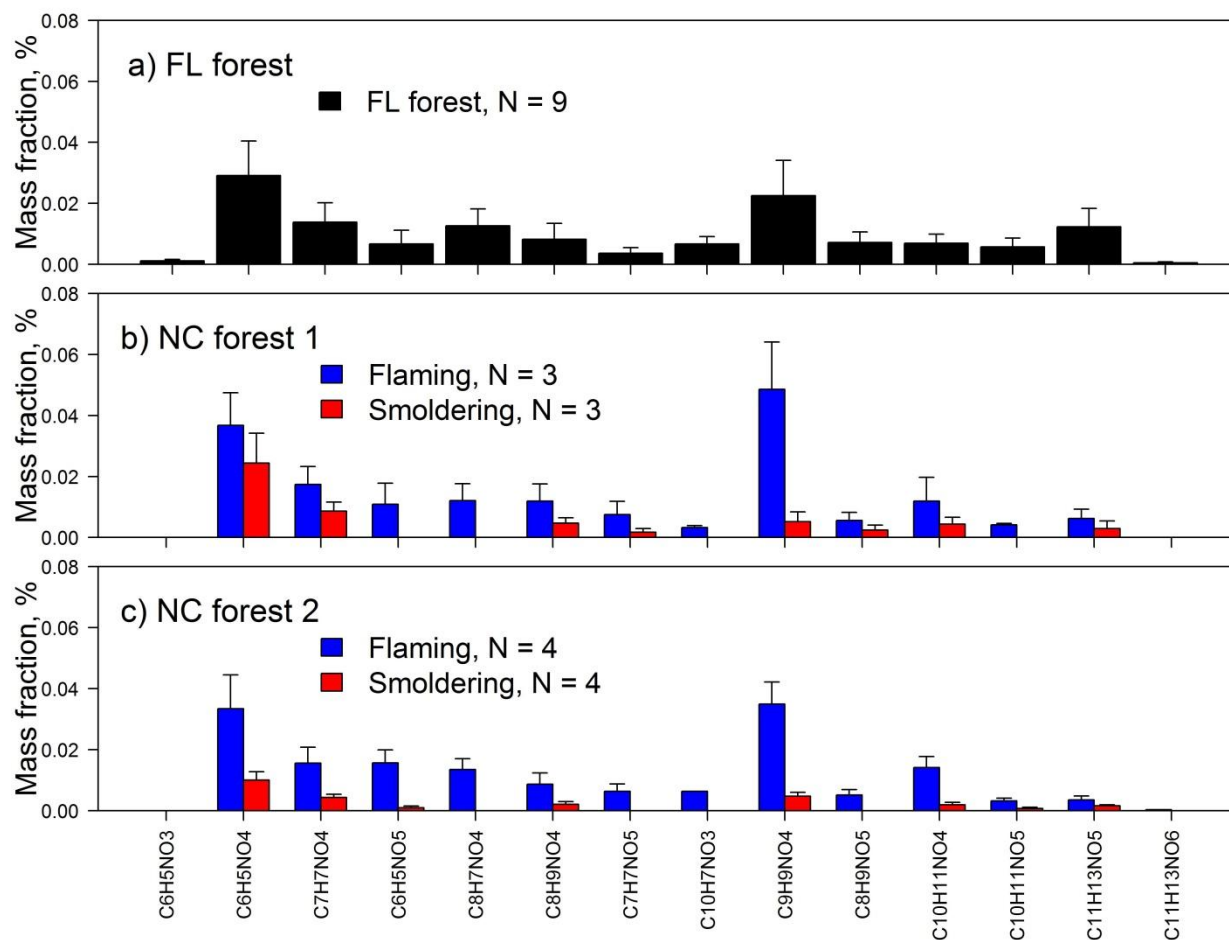


Figure 3. Relative mass contributions of identified N-containing aromatic compounds in BB samples collected during (a) FL forest, (b) NC forest 1 and (c) NC forest 2 experiments.

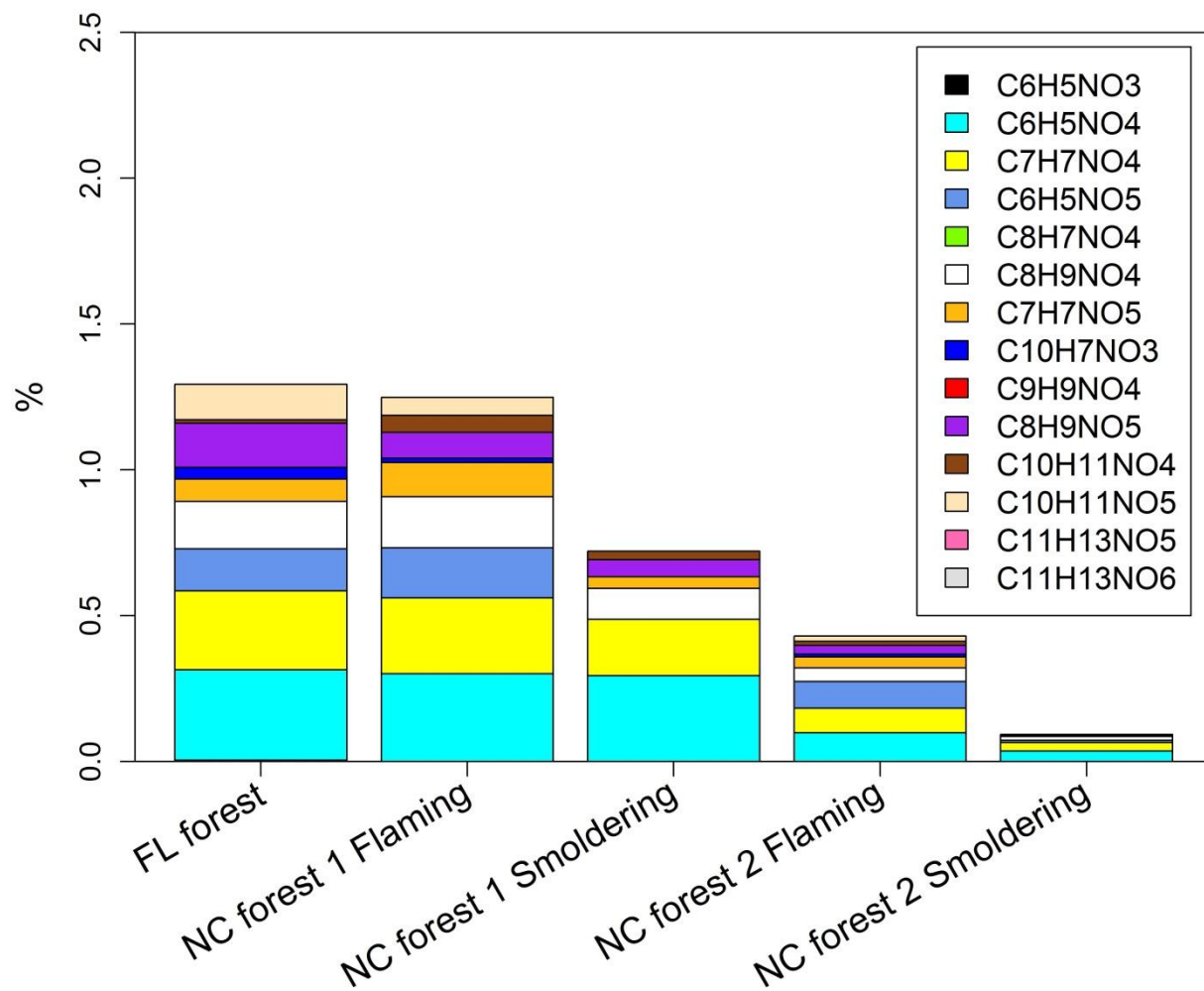


Figure 4. Average contributions (%) of N-containing aromatic compounds to Abs₃₆₅ of methanol extractable OC from laboratory biomass burning.